Different Mismatch Repair Deficiencies All Have the Same Effects on Somatic Hypermutation: Intact Primary Mechanism Accompanied by Secondary Modifications

By Nayun Kim,* Grazyna Bozek,‡ James C. Lo,‡ and Ursula Storb‡

*From the *Department of Biochemistry and Molecular Biology and the ‡Department of Molecular Genetics and Cell Biology, University of Chicago, Chicago, Illinois 60637*

Summary

Somatic hypermutation of Ig genes is probably dependent on transcription of the target gene via a mutator factor associated with the RNA polymerase (Storb, U., E.L. Klotz, J. Hackett, Jr., K. Kage, G. Bozek, and T.E. Martin. 1998. *J. Exp. Med.* 188:689–698). It is also probable that some form of DNA repair is involved in the mutation process. It was shown that the nucleotide excision repair proteins were not required, nor were mismatch repair (MMR) proteins. However, certain changes in mutation patterns and frequency of point mutations were observed in Msh2 (MutS homologue) and Pms2 (MutL homologue) MMR-deficient mice (for review see Kim, N., and U. Storb. 1998. *J. Exp. Med.* 187:1729–1733). These data were obtained from endogenous immunoglobulin (Ig) genes and were presumably influenced by selection of B cells whose Ig genes had undergone certain mutations. In this study, we have analyzed somatic hypermutation in two MutL types of MMR deficiencies, Pms2 and Mlh1. The mutation target was a nonselectable Ig-κ gene with an artificial insert in the V region. We found that both Pms2- and Mlh1-deficient mice can somatically hypermutate the Ig test gene at approximately twofold reduced frequencies. Furthermore, highly mutated sequences are almost absent. Together with the finding of genome instability in the germinal center B cells, these observations support the conclusion, previously reached for Msh2 mice, that MMR-deficient B cells undergoing somatic hypermutation have a short life span. Pms2- and Mlh1-deficient mice also resemble Msh2-deficient mice with respect to preferential targeting of G and C nucleotides. Thus, it appears that the different MMR proteins do not have unique functions with respect to somatic hypermutation. Several intrinsic characteristics of somatic hypermutation remain unaltered in the MMR-deficient mice: a preference for targeting A over T, a strand bias, mutational hot spots, and hypermutability of the artificial insert are all seen in the unselectable Ig gene. This implies that the MMR proteins are not required for and most likely are not involved in the primary step of introducing the mutations. Instead, they are recruited to repair certain somatic point mutations, presumably soon after these are created.

Key words: DNA mismatch repair • immunoglobulin genes • somatic hypermutation • transgenic mice

Immunoglobulin (Ig) genes are first rearranged in early B cell development through the V(D)J recombination process and then further modified upon antigenic stimulation through the somatic hypermutation process. The mutation process is active in the germinal center (GC)[1] of secondary lymphoid organs such as lymph nodes, the spleen, and Peyer's patches (1). Mutations accumulated in Ig genes, coupled with antigen-dependent clonal selection, result in affinity maturation. B cells that have acquired mutations in the Ig gene variable region leading to higher affinity antibodies are preferentially selected for further differentiation and proliferation (1). Somatic hypermutations primarily consist of single substitutions introduced to rearranged Ig genes and are confined to ~1.5 kb downstream of the transcription start site (for review see reference 2). There is also evidence for a strand bias that can be detected as there is an A over T bias (3), although in some cases such bias was not observed (4). Certain short sequences are hot spots of mutation, such as the AGY trinucleotide (5).

Transcription has been shown to be closely linked to the Ig somatic mutation process through the study of Ig transgenic mice. Notably, Peters and Storb demonstrated that

[1]*Abbreviations used in this paper:* GC, germinal center; MMR, mismatch repair; NER, nucleotide excision repair; SSR, simple sequence repeat.

mutation can be directed to the constant region of an Ig transgene by duplication of the Ig promoter just upstream of the constant region exon (6). In another study of transgenic mouse lines, Fukita et al. (7) showed that deletion of the promoter in an otherwise intact Ig transgene results in a greatly reduced mutation rate. In conjunction with earlier reports concerning the importance of Ig transcriptional enhancers in the mutation process (8), the findings suggest that the Ig somatic mutation process is coupled to the transcription process. It has been proposed that the molecular mechanism of the somatic hypermutation of Ig genes involves DNA repair processes in addition to transcription. One such proposed model invoked gratuitous transcription-coupled repair as a key step in the introduction of mutations (6). However, studies of human cell lines and mice deficient in nucleotide excision repair (NER) have shown that, although NER is known to be involved in transcription-coupled repair (9), it is not required for Ig somatic mutation (10–14).

Although NER is responsible for repairing DNA damage with bulky adducts such as UV photoproducts (15), postreplication mismatch repair (MMR) is responsible for correcting misincorporation or slippage errors introduced during the replication phase of the cell cycle (16). In *Escherichia coli*, three genes are essential for MMR function, *mutS*, *mutL*, and *mutH* (16). MutS, the protein that recognizes mispaired bases, forms a functional MMR complex with MutL and MutH. MutH is an endonuclease that recognizes hemimethylated DNA. This allows the correct repair of newly synthesized, unmethylated strands of DNA. In humans, mutations in homologues of *mutS* or *mutL* have been identified in patients with hereditary nonpolyposis colorectal cancer. The mouse *Msh2* gene (*mutS* homologue), *Mlh1* gene (*mutL* homologue), and *Pms2* gene (*mutL* homologue) have been individually studied in gene disruption experiments (17–19). These MMR-deficient mice show microsatellite instability, spontaneous tumors, and various sterility problems. Surprisingly, Mlh1 deficiency and Pms2 deficiency result in different types of spontaneous tumors and different types of sterility problems in spite of their biochemical function being very closely related. Recently, several labs have reported that mismatch-deficient mice, $Msh2^{-/-}$ or $Pms2^{-/-}$, display normal frequencies of Ig somatic hypermutation but an altered spectrum of mutations (13, 14, 20–22). Such results point to a possible role of the MMR mechanism in somatic hypermutations of Ig genes in the introduction, the repair, or the "fixing" of mutations. However, the previous studies of Ig mutation in MMR-deficient mice involved sequence analysis of endogenous Ig genes. Therefore, the question of altered mutation pattern is clouded by the issue of selection. To determine the direct effect of MMR deficiency on Ig somatic hypermutation, we have analyzed mutation patterns of a passenger transgene that can be targeted for Ig mutation but, due to a premature stop codon, does not interfere with selection. We have also compared the effect of *Mlh1* deficiency on somatic mutations in chronically stimulated Peyer's patch B lymphocytes to those in B lymphocytes in the spleen.

Materials and Methods

Mice. Mlh1 and Pms2 knockout mice were provided by Dr. R.M. Liskay (Oregon Health Sciences University, Portland, OR). Heterozygote males and females were bred and offspring were genotyped using a PCR-based method as previously described (17, 18). The mice were kept in a conventional mouse colony and are summarized in Table I. For the study of splenic GC B cells, mice were immunized twice by intraperitoneal injection of 2×10^8 SRBCs (ICN Biomedicals) on days 1 and 8 and killed 7 d after the second immunization.

Isolation of GC B Cells. Single cell suspensions from spleens or Peyer's patches were stained with PE-conjugated anti-B220 (CD45R) antibody (GIBCO BRL), FITC-conjugated PNA (Sigma Chemical Co.), and FITC-conjugated GL7 antibody (PharMingen). $B220^+/(PNA\ GL7)^{high}$ cells were isolated using FACStar^{plus} (Becton Dickinson). For the study of the Vk167/PEPS transgene in splenic GC B cells, the depletion of subsets of cells was carried out before FACS® as described by Jacobs et al. (13) except for the following changes. T cells ($Thy1.2^+$), B1 cells ($CD5^+$), macrophages ($Mac3^+$), and virgin B cells (IgM^+, IgD^+) were depleted from the splenic cells by the magnetic-activated cell sorting method. A single cell suspension was first incubated with biotinylated antibodies to Thy1.2, CD5, Mac3, sIgM, or sIgD (PharMingen) and then incubated with streptavidin-coated magnetic beads (Dynal). Cells bound by beads were depleted by a strong magnet and cells free of beads were used in GC B cell isolation as described above.

PCR Amplification. The synthesis of cDNA was carried out as suggested in the Superscript II kit (Stratagene) using oligo d(T)16 primer (PE Applied Biosystems). Amplification of the VH11 gene from the cDNA was carried out as previously described by Rogerson (23).

560-bp fragments of the Vk167/PEPS transgene containing EPS sequences were amplified with Pfu DNA polymerase (Stratagene) and 5′ primer Vk3B (5′ GTCAGTGGGGATATTGTGATAACC) and 3′ primer EKVK2 (5′ TCAACTGATAATGAGCCCTC). Both primers were phosphorylated in reactions containing 1 mM ATP and T4 polynucleotide kinase (New England Biolabs) before the PCR reaction. PCR conditions were 30 cycles of 94°C for 15 s, 62°C for 20 s, and 72°C for 30 s.

All PCR-generated fragments were cloned by blunt end ligation into the Srf1 site of pCRscript (Stratagene) or the Sma1 site of pKS(+). Ligation reaction mixtures contained T4 DNA ligase and either SrfI or SmaI (New England Biolabs) in order to minimize vector religation.

EcoRV/PvuII Restriction Site Analysis. Analysis of the EPS in Vk167/PEPS transgene has been previously described (24). In brief, each plasmid clone with the 560-bp fragment insert of the transgene was amplified using primers Vk8B (5′ GTTTCAGCTCCAGCTTG) and Vk9B (5′ CTCCTCAGCTCCTGATC) (35 cycles of 94°C for 20 s, 60°C for 30 s, and 72°C for 30 s). The PCR product was digested with either EcoRV or PvuII (New England Biolabs) and separated on a nondenaturing 18% polyacrylamide/5% glycerol gel and visualized by ethidium bromide staining. Mutation at one of the restriction sites results in disappearance of smaller bands and/or appearance of larger bands (see Fig. 2 B).

Single Strand Conformation Polymorphism. Single strand conformation polymorphism (SSCP) analysis was carried out according to Orita et al. (25) with the following modifications in the protocol: plasmid DNA was amplified with Vk3B and EkVk2 primers in 10 μl reactions containing PFU DNA polymerase, 2 mM of each dNTP, and 1 μCi of [α-^{32}P]dCTP. PCR conditions were as described above. PCR products were digested with restriction

Table I. *Mice Used in This Study*

Experiment	Mice					
	Genotype	No.	Name*	Sex	Age	Genetic background‡
S107 analysis	$Mlh1^{-/-}$	1	E717	male	11 wk	B6
	$Pms2^{-/-}$	1	E661	male	8 wk	B6
EPS analysis, spleen	Wt	3	#63	male	10 wk	(CD1×B6)F1
			E834 ($Pms2^{+/-}$)	male	14 wk	~25% CD1
			E840 ($Pms2^{+/+}$)	male	14 wk	~25% CD1
	$Mlh1^{-/-}$	2	E976	male	12 wk	~12.5% CD1
			A005	male	12 wk	~12.5% CD1
	$Pms2^{-/-}$	2	E931	male	9 mo	~25% CD1
			E842	female	6.5 mo	~25% CD1
EPS analysis, Peyer's patches	Wt	1	A144 ($Mlh1^{+/+}$)	male	14 wk	~12.5% CD1
	$Mlh1^{-/-}$	2	A145	female	14 wk	~12.5% CD1
			A146	male	14 wk	~12.5% CD1

The EPS founder (PEPS4; reference 24) was CD1 background. It was crossed with B6, as were its offspring. For the crosses with $Pms2^{+/-}$ mice (B6), a (CD1-PEPS4 × B6)F1 was used in the first generation and brother–sister mating was used in subsequent crosses to result in $Pms2^{-/-}$ (or $Pms2^{+/-}$, or $Pms2^{+/+}$) PEPS4 mice. For the crosses with $Mlh1^{+/-}$ mice, a (CD1-PEPS4 × B6)F1 × B6 mouse was used in the first generation and brother–sister (or cousin–cousin) mating was used in the subsequent crosses to result in $Mlh1^{-/-}$ (or $Mlh1^{+/+}$) PEPS4 mice.
*Organs (spleens or Peyer's patches) of mice marked by brackets were pooled.
‡The $Mlh1^{-/-}$ and $Pms2^{-/-}$ mice originated in strain 129/Sv and had been exhaustively crossed with C57BL/6 (B6) mice.

endonuclease TaqαI (New England Biolabs) at 65°C, which results in two fragments of 300 and 260 bp, respectively. Digested PCR products were diluted with dilution solution (10 mM EDTA, 0.1% SDS) and stop solution (95% formamide, 20 mM NaOH, 20 mM EDTA, 0.15% bromophenol blue, and 0.15% xylene cyanol). The mixture was denatured by incubation at 98°C for 10 min and quick chill on ice. Resolution was carried out by electrophoresis through a 6% polyacrylamide/10% glycerol gel at 6 W for 17–19 h. The gel was dried and exposed to Kodak X OMAT film (Eastman-Kodak Co.).

Sequencing. Sequencing was carried out either manually using the Sequenase II Dideoxy Terminator Sequencing kit (United States Biochemical Corp.) or by University of Chicago Cancer Research Center DNA Sequencing Facility using ABI Prism model 377 sequencer (Applied Biosystems, Inc.). The sequencing primers T7, T3, or reverse primer were used. The reverse primer (5′ GGAAACAGCTATGACCATG 3′) is a primer just upstream of the T3 primer in the multiple cloning site of pKSII(+) or pCRSCRIPT.

Microsatellite Analysis. Oligonucleotide primers (D4Mit42F and D4Mit42R) specific to simple sequence repeat (SSR) locus D4Mit42 were obtained from Research Genetics. Before the PCR reaction, the D4Mit42F primer was phosphorylated with T4 Polynucleotide Kinase (New England Biolabs) and [γ-^{32}P] ATP. PCR reaction contained 1 pmol each of labeled D4Mit42F primer and unlabeled D4Mit42R primer, 0.2 mM of each dNTP, 0.25 U of Taq polymerase, and 20–40 pg of DNA in a total vol of 10 μl. The PCR conditions were 32 cycles of 15 s at 94°C, 30 s at 55°C, and 30 s at 72°C. The products were separated on a 6% polyacrylamide denaturing sequencing gel and exposed to phosphor screen (Molecular Dynamics). The image was visualized by scanning with a Storm 860 scanner and analyzed by ImageQuant software (Molecular Dynamics).

Results

Normal Somatic Hypermutations in Endogenous Heavy Chain Variable Gene. Somatic hypermutation of an endogenous Ig gene was studied in knockout mice twice immunized with SRBCs. $B220^{+}PNA^{hi}$ B cells, which represent the GC B cell compartment, were isolated from spleens of $Mlh1^{-/-}$ or $Pms2^{-/-}$ mice. RNA was extracted from these cell populations and the VH11 gene, which is a member of the S107 family of heavy chain variable genes, was amplified by the reverse transcription PCR method and cloned for sequencing. In addition to the S107 family gene–specific primer, a primer specific to the γ constant region was used in amplification so that only the VH11 gene sequences from activated B cells that have switched to the γ constant region would be represented. Sequence analysis showed normal frequencies of somatic hypermutation in $Pms2^{-/-}$ as well as in $Mlh1^{-/-}$ mice (Fig. 1). The frequencies of somatic hypermutation in the clones analyzed were 0.7% in $Pms2^{-/-}$ mice and 1% in $Mlh1^{-/-}$ mice. Comparable mutation frequencies were previously reported for VHS107 genes in GC B lymphocytes of wild-type mice immunized in the same way (23). Incidentally, five out of six $Mlh1^{-/-}$ clones sequenced were potentially related clones containing the same VDJ junction and

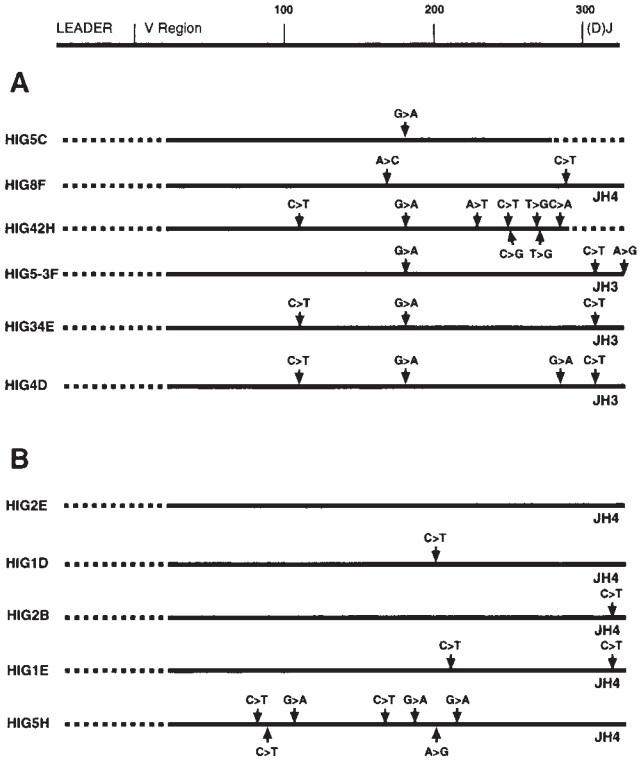

Figure 1. Analysis of VH11 gene mutations. A VH11 sequence is represented by each line. The locations of mutations are indicated by arrows with the specific nucleotide change written above each arrow. The solid line represents the sequenced region and the dotted line represents the unanalyzed sequence. All clones represented in this figure are of the IgG isotype. (A) VH11 clones from $Mlh1^{-/-}$ mice. (B) VH11 clones from $Pms2^{-/-}$ mice.

sharing some identical mutations. As a control, the VH11 gene was amplified from a $B220^{+}PNA^{lo}$ population using VH11 and μ constant region–specific primers and no mutation was found in five sequenced clones (data not shown).

MLH1- or PMS2-deficient Mice Have a Near Normal Frequency of Mutation But Altered Patterns. By analysis of VH11 gene clones, we have confirmed that the disruption of the *Mlh1* gene or of the *Pms2* gene does not have a significant effect on the frequency of Ig somatic mutation. To address the issue of altered mutation spectra without the complication of selection, we decided to pursue the analysis of a passenger transgene in the MMR-deficient strains of mice. The Vk167/PEPS transgene contains an insertion of a 108-bp artificial sequence within a rearranged κ light chain transgene (Fig. 2 A). The insertion, termed EPS, contains multiple EcoRV and PvuII sites that allow the detection of mutation by restriction fragment length variance. Of 108 bp in EPS, 76 bp lie in EcoRV or PvuII recognition sites. Mutation at any one of these positions results in the loss of the particular restriction site (Fig. 2 B). Previous study of one transgenic mouse line, PEPS4, which carries four copies of the Vk167/PEPS transgene, showed that this transgene can be targeted for Ig somatic hypermutation (24, 26). Furthermore, the 108-bp EPS portion of the transgene showed a mutation frequency ~10 times higher than the rest of the transgene sequences analyzed (Table II) (24, 26).

Mice heterozygous for *Mlh1* or *Pms2* disruption were bred with the PEPS4 line of transgenic mice. Mice homozygous for the disrupted allele and positive for the transgene were immunized twice with SRBCs and killed 7 d after the second immunization for harvest of the spleens. We enriched for activated GC B lymphocytes from splenic cells by depleting T cells, B1 cells, macrophages, and virgin B cells. Activated GC B lymphocytes were isolated from this enriched population by fluorescence-activated cell sorting. A part of the transgene was amplified with Pfu high fidelity DNA polymerase from the DNA of these GC B cells and cloned for analysis. Identification of mutations in the EPS was carried out as previously described. Approximately 1 out of 30 clones analyzed was identified to have mutations in one of the restriction sites. Subsequently, ~560 bp of each transgene clone including EPS and flanking Ig gene sequences were sequenced. A total of 26 clones were sequenced from $Mlh1^{-/-}$ mice and 15 clones from $Pms2^{-/-}$ mice with total numbers of mutations identified being 41 and 27 respectively (Fig. 3 and Table II). Mutation frequencies were 2.9×10^{-3} for $Mlh1^{-/-}$ mice and 3.3×10^{-3} for $Pms2^{-/-}$ mice. These are approximately twofold lower than 4.7×10^{-3}, which is the frequency we observed in wild-type mice in a previous study ($P < 0.0005$ for $Mlh1^{-/-}$ and $Pms2^{-/-}$) (26). We did not find increased

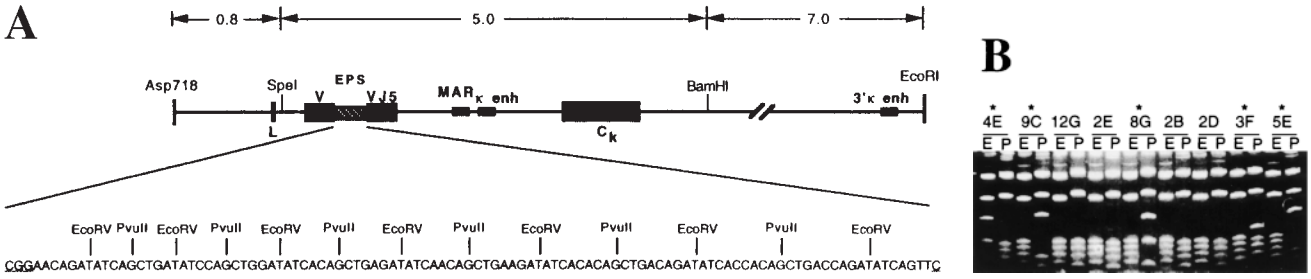

Figure 2. Map of the Vk167/PEPS transgene and EPS analysis. (A) Vk167/PEPS transgene and sequence of the EPS insert. The restriction sites within the EPS are indicated. (B) An example of PAGE from an EPS analysis. PCR products from nine clones were digested with EcoRV (E) or PvuII (P) and resolved in 18% acrylamide gel. Unmutated clones (12G, 2E, 2B, and 2D) show two large bands flanking the EPS region and ladders of small bands. In case of EcoRV digestion, the small bands are 20, 18, 16, 14, 12, and 10 bp (12- and 10-bp bands are invisible here). In case of PvuII digestion, the small bands are 19, 17, 15, 13, and 11 bp (11-bp bands are invisible). An asterisk indicates mutated clones. Clone 8G, for example, has a mutation in the fourth PvuII site (PD), so the 15- and 17-bp bands are gone and a 32-bp band has appeared.

Table II. *Somatic Mutation in Vk167/PEPS Transgene from Splenic GC B Cells*

	Wild-type*	Mlh1$^{-/-}$	Pms2$^{-/-}$
No. of clones	46	26	15
Total No. of mutations	113	41	27
Mutation frequency in EPS (10^{-3})	17.0	12.4	12.0
Mutation frequency in flank (10^{-3})	1.7	.75	1.3
Mutation frequency total (10^{-3})	4.7	2.9	3.3
Tandem mutations	2	0	1
% mutations from A‡	27.3	29.0	22.7
% mutations from T‡	15.9	2.3	0
% mutations from C‡	35.1	32.5	17.3
% mutations from G‡	21.7	36.2	60.0

See Table I for the properties of the mice used.
*Data in this column are from reference 26. Only those mutations within the transgene sequences from nucleotides 408 to 916 were considered for this tabulation. For the nucleotide numbers, see Fig. 3.
‡Percentage of mutations from each nucleotide are corrected for the base composition.

numbers of tandem mutations in Pms2$^{-/-}$ mice in contrast to the report by Winter et al. (14). The proportion of mutations from G and C nucleotides is significantly greater in Mlh1$^{-/-}$ and Pms2$^{-/-}$ mice than in wild-type mice. Increased mutations from G and C nucleotides have been reported in Msh2$^{-/-}$ mice (13, 20) but in analogous studies comparable alterations are not found in Pms2$^{-/-}$ or Mlh1 mice (14, 27). This discrepancy is unexplained. Our analysis of Mlh1$^{-/-}$ and Pms2$^{-/-}$ mice indicates that the increase in mutations from G and C nucleotides is the effect of the lack of MMR function in general and not the effect of the lack of functional mispair binding proteins such as Msh2/3/6.

The Effect of Mlh1 Disruption Is More Pronounced in Peyer's Patch B Cells. Frey et al. (22) recently reported that Msh2 deficiency interferes with the accumulation of high numbers of mutations in Peyer's patch GC B cells. We wanted to ascertain whether the effect of disruption of the *Mlh1* gene is similar in chronically stimulated B cells from Peyer's patches. 14-wk-old littermates, Mlh1$^{-/-}$ and Mlh1$^{+/+}$, were used in the study. The mice were killed and Peyer's patches were dissected out from the intestines of these mice. GC B cells were then isolated by flow cytometry. Cloning and analysis of the EPS transgene were carried out as for the splenic GC B cells. In addition to restriction fragment length variance analysis, single strand conformation polymorphism (SSCP) analysis was carried out in identifying clones with somatic mutations. For wild-type mice, a total of 82 mutations from 24 clones were identified for a mutation frequency of 6.5×10^{-3} (Fig. 4 A). This mutation frequency represents an ~38% increase from the mutation frequency found in the splenic GC B cells of wild-type mice. The total number of mutations found in Mlh1$^{-/-}$ was 53 in 29 clones analyzed (Fig. 4 B). The mutation frequency was 3.5×10^{-3}, which is not significantly different from that of the splenic GC B cells of Mlh1$^{-/-}$ mice (2.9×10^{-3}) but is twofold less than that of Peyer's patch cells of wild-type mice ($P = 0.02$) (Table III). An increase in mutations from G and C nucleotides was again observed in the Peyer's patch B cells of Mlh1$^{-/-}$ mice. We also noted that clones with high numbers of mutations were much reduced in Mlh1$^{-/-}$ mice (Fig. 5). About 65% of mutated clones from Mlh1$^{-/-}$ contained a single mutation, whereas ~75% of the mutated clones from wild-type mice contained multiple mutations, up to 16 mutations per clone. In their analysis of Msh2$^{-/-}$ mice, Frey et al. (22) observed a great increase in the microsatellite instability in Peyer's patch GC B cells (PNA^{hi}) compared with non-GC B cells from Peyer's patches (PNA^{lo}). We analyzed the stability of CA nucleotide repeat microsatellites at the SSR D4Mit42 locus in Mlh1$^{-/-}$ mice, and observed that Peyer's patch GC B cells contained deletions or insertions in the D4Mit42 locus at a frequency of 11.5% (9 out of 78) (Fig. 6). Non-GC B cells showed a microsatellite instability at a three times lower frequency of 3.6% (3 out of 84). It seems that the accumulation of mutations in Peyer's patch cells is affected by *Mlh1* disruption as well as by *Msh2* disruption.

Discussion

There Are No Gross Immune Defects in Mlh1$^{-/-}$ or Pms2$^{-/-}$ Mice. MMR-deficient mice, Msh2$^{-/-}$, Mlh1$^{-/-}$, or Pms2$^{-/-}$, have severe health problems relating to the gene disruption (17–19). In all of these, a high incidence of cancer and a dramatic increase in microsatellite instability is noted. Additionally, *Mlh1* or *Pms2* gene disruption leads to abnormalities in meiosis and thus to fertility problems. However, we did not find any gross defects in the immune function of Mlh1$^{-/-}$ or Pms2$^{-/-}$ mice that might compromise the somatic hypermutation process. The levels of serum Igs of various isotypes were normal in the Pms2^{-} and Mlh1^{-} mice (data not shown), thus isotype switching appeared to be normal. Also, when compared with the serum of wild-type mice immunized at the same time, Mlh1$^{-/-}$ or Pms2$^{-/-}$ mice showed no discernible defect in immune response to the heterologous antigens in SRBCs (data not shown). Early B cell development in bone marrow was studied by FACS® analysis. We did not see any consistent difference in populations of B220^{lo} or B220^{hi} cells or in IgM/IgD double positive cells (data not shown). No significant differences in GC cells as assayed were noted; we found similar proportions of B220^{+}PNA^{hi} cells in the spleens as well as the Peyer's patches of wild-type or MMR-deficient mice (data not shown). These observations are in contrast to the recent finding of defective immune responses in Msh2 knockout mice (21, 28). It remains to be determined whether the differences are due to the type of MMR defect studied (*mutS* homologue

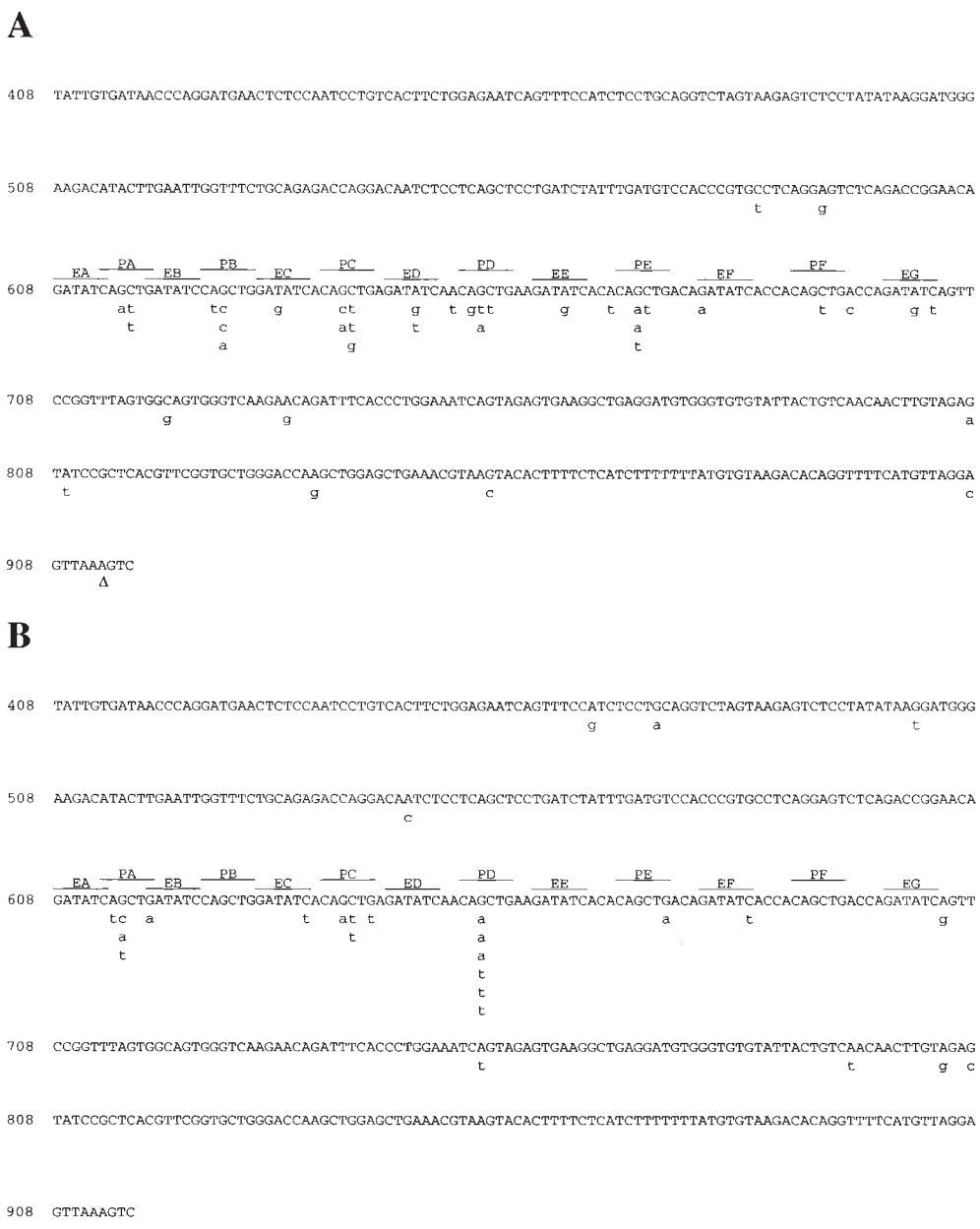

Figure 3. Analysis of Vk167/PEPS transgene mutations in splenic GC B lymphocytes. The original transgene sequences from NT 408 to 916 are shown in uppercase letters. Mutations are indicated in lowercase letters. The restriction sites within the EPS are indicated by a line over the sequence. E is an EcoRV and P is a PvuII site. A Δ denotes a deletion. (A) Mutations from Mlh1$^{-/-}$ mice. (B) Mutations from Pms2$^{-/-}$ mice.

versus *mutL* homologue), the immunization schedules, or perhaps background genes of the mouse strains studied.

Intrinsic Characteristics of Somatic Hypermutation Remain Unaltered in MMR-deficient Mice. As with wild-type mice, we found in the analysis of MMR-deficient mice that mutations from A were much more frequent than were mutations from T (Tables II and III). This bias of A over T has been seen in most studies of Ig somatic hypermutation and suggests that there is a strand bias and a nucleotide preference (A or T) that are intrinsic to the mutation mechanism (3). From previous study of the Vk167/PEPS transgene, it was noted that the EPS fragment of the transgene that contains six PvuII sites and seven EcoRV sites was an order of magnitude more mutable than the rest of the VJ region (26). We have proposed that the hypermutability may be related to the highly stable RNA secondary structures predicted in the EPS region. The striking correlation between the RNA stem formation energy and the location of highly mutated sequences led us to suggest that the mutations could be directed by the secondary structure of nascent RNA transcripts and perhaps by the RNA polymerase pausing due to such RNA secondary structure (26). In MMR-deficient mice, we found that the hypermutability of the EPS is intact (Tables II and III). Thus, the hypermutability of the EPS sequence in wild-type and MMR-deficient mice is most likely the consequence of the primary mechanism of the introduction of the mutations (see below). We also found that in Mlh1$^{-/-}$ mice, just as in wild-type mice, there exists a mutation preference for certain nucleotides within the EcoRV or PvuII sites (Fig. 7). Not enough data from Pms2$^{-/-}$ mice were accumulated for analogous consideration. Among the six nucleotides within the EcoRV sites,

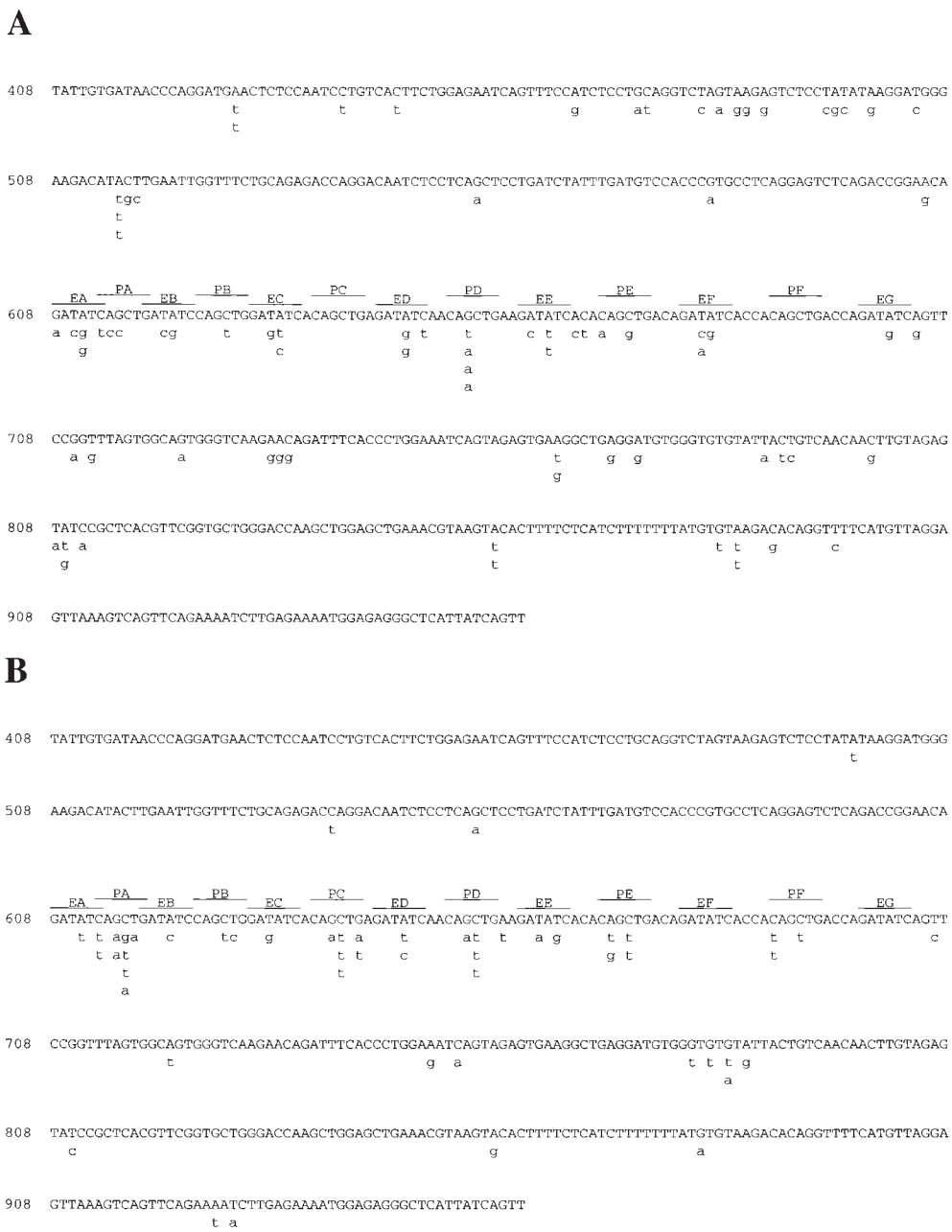

Figure 4. Analysis of Vk167/PEPS transgene mutations in Peyer's patch GC B lymphocytes. (A) Mutations from wild-type mice. (B) Mutations from Mlh1$^{-/-}$ mice.

T and A nucleotides at positions 3 and 4, respectively, are much more frequently mutated than are the remaining four nucleotides. Similarly, within the PvuII sites, the G nucleotide at position 3 and the C nucleotide at position 4 are much more frequently mutated. These preferred nucleotides within the restriction sites correlate with the sequences of known hot spots as described by Smith et al. (5). The di- and trinucleotide hot spots listed by Smith et al. were derived from mutations in noncoding (therefore unselectable) regions of Ig genes and must reflect the targeting preference ingrained in the Ig mutation mechanism. Rada et al. (21) found that mutations were increasingly focused on the mutational hot spots in Msh2$^{-/-}$ mice. The proportion of mutations found at the hot spots was elevated from 8.2% in wild-type mice to 25.1% in Msh2$^{-/-}$ mice. Our analysis of Mlh1- or Pms2-deficient mice showed the persistence of mutation hot spots within the EPS but not a noticeable increase in hot spot focusing. The proportion of mutations found in the hypermutable EPS in wild-type mice was ~40%, and the frequencies in Mlh1- and Pms2-deficient mice were 51 and 44%, respectively. The discrepancy with Rada et al. (21) could be due to the fact that the mutated bases in their hot spots were biased toward G and C, whereas ours were balanced for A, T, G, and C (Fig. 7). Perhaps GC-rich hot spots are treated differently from AT-rich hot spots in the primary mutation mechanism.

Thus, our analysis of Mlh1$^{-/-}$ and Pms2$^{-/-}$ mice shows that several signature properties of Ig somatic hypermuta-

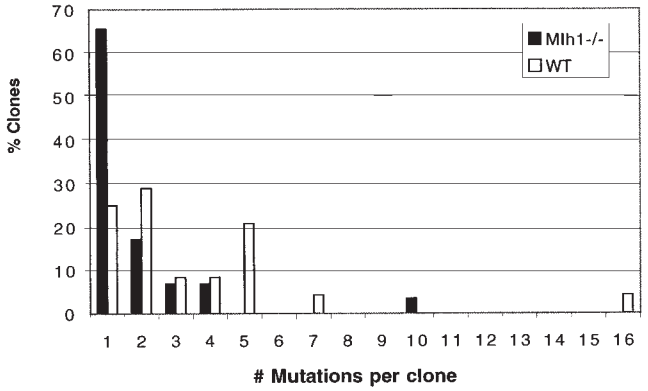

Figure 5. Mutation accumulation in Peyer's patch B cells. Each bar represents the percentage of Vk167/PEPS clones with a given number of mutations. The distribution is calculated from the total number of clones analyzed as indicated in Table III.

tion remained unchanged in these MMR-deficient mice. A preference for targeting A over T (in the case of the non-transcribed strand of DNA) or of targeting T over A (in the case of the transcribed strand), a strand bias, mutational hot spots, and the hypermutability of the EPS are all observed in the analysis of the unselectable Vk167/PEPS transgene in the MMR-deficient backgrounds. The implication is that MMR proteins are not required for the primary step of introducing Ig somatic hypermutations, and also, that the absence of functional MMR does not alter the primary mechanistics of somatic hypermutation.

Mutation Spectra of Mlh1$^{-/-}$ Mice Are Similar to Those of Msh2$^{-/-}$ Mice. Recently, a number of labs reported that MMR deficiency in mice results in altered mutation spectra of Ig gene somatic hypermutation. One of the conflicting points among these reports is that even though both Msh2 and Pms2 are essential factors in MMR function, Msh2 and Pms2 deficiency reportedly carry different consequences for Ig hypermutation. Phung et al. (20) reported increased mutation from G and C nucleotides in Msh2$^{-/-}$ mice, whereas an increase in tandem mutations was noted in Pms2$^{-/-}$ mice (14). This has led to speculation that the presence or absence of certain functional mismatch binding complexes (Msh2/3 heterodimers or Msh2/6 heterodimers) might differentially affect the final outcome of the somatic hypermutation process (22, 29). In addition, evidence from knockout mice suggests that *Msh2*, *Mlh1*, or

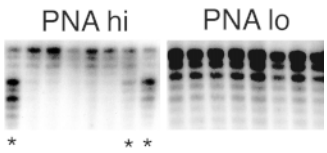

Figure 6. Microsatellite instability in Peyer's patch B lymphocytes of Mlh1$^{-/-}$ mice. PNA^{hi} indicates the B220^{+}PNA^{hi} cell population (GC B cells) and PNA^{lo} indicates the B220^{+}PNA^{lo} cell population (non-GC B cells). Each lane contains the product of a single PCR reaction with about one cell equivalent of genomic DNA as template. Primers specific to D4Mit42 SSR locus are used in the PCR. Three out of nine separate reactions from the PNA^{hi} population show instability in CA repeats (indicated by an asterisk), as evidenced by the appearance of the shorter PCR product. All reactions from the PNA^{lo} population show the PCR products of the correct length (102 nucleotides).

Table III. *Somatic Mutation in Vk167/PEPS Transgene from Peyer's Patch GC B Cells*

	Wild-type	Mlh1$^{-/-}$
No. of clones	24	29
Total No. of mutations	82	53
Mutation frequency in EPS (10^{-3})	13.5	12.9
Mutation frequency in flank (10^{-3})	4.9	1.4
Mutation frequency total (10^{-3})	6.5	3.5
% mutations from A*	43.7	21.2
% mutations from T*	17.2	13.2
% mutations from C*	22.3	43
% mutations from G*	16.8	22.6

See Table I for the properties of mice used.
*Percentage of mutations from each nucleotide are corrected for the base composition.

Pms2 gene products are involved in more than postreplicative DNA MMR and perhaps each of these factors might be involved in some unique function. For example, Msh2-deficient mice are fertile, whereas Mlh1 deficiency leads to both male and female infertility and Pms2 deficiency leads only to male infertility (17, 18). This may imply that Mlh1 and Pms2 perform a role, at least in meiosis, independent of Msh2 and perhaps independent of each other. However, we have found that disruption of the MutL homologues Mlh1 and Pms2 result in altered mutation spectra very similar to those seen in Msh2$^{-/-}$ mice. There is a noticeable increase in mutations arising from G or C nucleotides in both Mlh1$^{-/-}$ and Pms2$^{-/-}$ mice. On the other hand, we did not observe an increase in tandem mutations in our analysis of Pms2$^{-/-}$ mice. This new evidence suggests that the altered spectra of mutations, that is, the increase in mutations from G and C nucleotides, are due to the absence of DNA

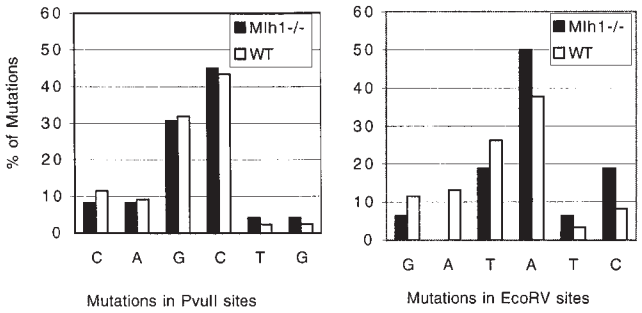

Figure 7. Mutation distribution within EcoRV or PvuII sites of the EPS sequence. Mutations from all six PvuII sites and all seven EcoRV sites are combined. Each bar represents the percentage of mutations at the specific location within the restriction recognition site out of total mutations. For example, the percentage of mutation at G nucleotide at position 3 of the PvuII site equals the number of mutations at G in all PvuII sites divided by the number of total mutations. Data from the analysis of splenic GC B cells and the analysis of Peyer's patch GC B cells were combined for this figure.

MMR function in general and not to the loss of any divergent function of any one of the MMR proteins. Another similarity between Msh2$^{-/-}$ and Mlh1$^{-/-}$ mice is the absence of highly mutated clones among Peyer's patch B cells. Frey et al. (22) suggested that the dramatic increase in microsatellite instability in Peyer's patch GC B cells observed in Msh2$^{-/-}$ mice is responsible for the lack of the accumulation of mutations. Our observation of the increase in microsatellite instability in Peyer's patch GC B cells of Mlh1$^{-/-}$ mice supports this proposal. GC B cells in Peyer's patches are highly proliferative and so the DNA damage (such as microsatellite instability) due to MMR deficiency could accumulate to a high degree, causing elimination of GC B cells after fewer rounds of mutation compared with wild-type mice. The effect of microsatellite instability and accumulative DNA damage is not as pronounced in splenic GC B cells. In spleen, GCs form in response to a recent antigenic stimulation and exist only for a short time ($\sim$3 wk), whereas in Peyer's patches the presence of food and bacterial antigens lead to chronic stimulation of GC B cells (1).

How Is MMR Involved in Ig Gene Somatic Hypermutation? During normal DNA replication, errors are corrected first by the proofreading activity of the DNA polymerase itself and then by postreplication DNA MMR. Postreplication MMR would not affect somatic mutation patterns unless the point mutations were introduced during S phase DNA replication. Recent evidence is strong that somatic mutation occurs during transcription (6, 8). There is no real evidence that it occurs during the S phase of the cell cycle. However, MMR proteins also seem to be involved in transcription-coupled repair of UV-damaged DNA in association with the NER process in *Escherichia coli* and in humans (30, 31). Mismatch-deficient human cell lines from hereditary nonpolyposis colorectal cancer patients lack the preferential repair of the transcribed strand of DNA (30). This implies that the MMR function may be present during interphase of the cell cycle and can function apart from the DNA replicative machinery. Several possible ways by which the MMR mechanism can contribute to the somatic hypermutation of Ig genes have been discussed previously. First, as Cascalho et al. (32) proposed, it can act to "fix" the mutations introduced in one of the strands by correcting the wrong strand of DNA. Mismatch repair deficiency, in this case, would lead to much reduced somatic hypermutation frequencies. However, several reports, including ours presented here, noted that no drastic decrease in mutation frequency exists in Msh2$^{-/-}$, Pms2$^{-/-}$, or Mlh1$^{-/-}$ mice. On the other hand, MMR might normally be downregulated in the GC B lymphocytes so as to allow the mutations to go uncorrected. The fact that somatic hypermutation occurs in MMR-deficient mice is compatible with this proposal. However, the mutation spectrum should be unchanged and the mutation frequency should be increased rather than decreased in these knockout mice if MMR were simply decreased in the course of the normal Ig somatic hypermutation process. The altered mutation spectra in MMR-deficient mice were clearly observed by several labs using several different systems: Vλ1 gene sequences from λ1^{+} memory B cells of nitrophenyl-chicken γ-globulin–immunized mice (13), rearranged VkOX1 gene sequences from the spleen of oxazolone-immunized mice (20), the JC intronic region of rearranged heavy chain genes in Peyer's patch PNA^{hi} cells (22), and, in this study, an unselectable transgene with a hypermutable insert both in spleens of SRBC-immunized mice and in Peyer's patches of old mice. Furthermore, recent reports indicated that MMR activity, as measured in an in vitro assay, is normal in isolated human centroblast cells (33) that are equivalent to GC (B220^{+}PNA^{hi}) B cells in mice. Thus, it is unlikely that downregulation of MMR is a normal mechanism to induce/enhance somatic hypermutation.

The fact that the mutation spectrum is altered in a very similar way in Msh2$^{-/-}$, Mlh1$^{-/-}$, and Pms2$^{-/-}$ mice suggests that an active MMR complex is present in GC B lymphocytes of normal mice and that it influences the outcome of somatic hypermutation by preferentially correcting some of the mutations introduced.

We thank Michael Liskay for the gift of MMR-deficient mice; Julie Auger for help with flow cytometry; and Kevin Fuller and Nancy Michael for comments on the manuscript.

This work was supported by National Institutes of Health (NIH) grant GM38649. N. Kim was partially supported by NIH training grant GM07183. The DNA sequencing facility is supported by the University of Chicago Cancer Center support grant P30 (A14599).

Address correspondence to Ursula Storb, Department of Molecular Genetics and Cell Biology, University of Chicago, 920 E. 58th Street, Chicago, IL 60637. Phone: 773-702-4440; Fax: 773-702-3172; E-mail: stor@midway.uchicago.edu

Submitted: 29 January 1999 Revised: 21 April 1999 Accepted: 6 May 1999

References

1. Kelsoe, G. 1995. The germinal center reaction. *Immunol. Today*. 16:324–326.
2. Storb, U. 1996. The molecular basis of somatic hypermutation of immunoglobulin genes. *Curr. Opin. Immunol.* 8:206–214.
3. Storb, U., A. Peters, E. Klotz, N. Kim, H.M. Shen, K. Kage, and B. Rogerson. 1998. Somatic hypermutation of immu-

noglobulin genes is linked to transcription. *Curr. Top. Microbiol. Immunol.* 229:11–19.
4. Doerner, T., H.-P. Brezinschek, R. Brezinschek, S. Foster, R. Domiati-Saad, and P. Lipsky. 1997. Analysis of the frequency and pattern of somatic mutations within nonproductively rearranged human variable heavy chain genes. *J. Immunol.* 158:2779–2789.
5. Smith, D., G. Creadon, P. Jena, J. Portanova, B. Kotzin, and L. Wysocki. 1996. Di- and trinucleotide target preferences of somatic mutagenesis in normal and autoreactive B cells. *J. Immunol.* 156:2642–2652.
6. Peters, A., and U. Storb. 1996. Somatic hypermutation of immunoglobulin genes is linked to transcription initiation. *Immunity*. 4:57–65.
7. Fukita, Y., H. Jacobs, and K. Rajewsky. 1998. Somatic hypermutation in the heavy chain locus correlates with transcription. *Immunity*. 9:105–114.
8. Betz, A., C. Milstein, R. Gonzalez-Fernandes, R. Pannell, T. Larson, and M. Neuberger. 1994. Elements regulating somatic hypermutation of an immunoglobulin κ gene: critical role for the intron enhancer/matrix attachment region. *Cell*. 77:239–248.
9. Hanawalt, P.C. 1994. Transcription-coupled repair and human disease. *Science*. 266:1957–1958.
10. Kim, N., K. Kage, F. Matsuda, M.-P. Lefranc, and U. Storb. 1997. B lymphocytes of xeroderma pigmentosum or Cockayne syndrome patients with inherited defects in nucleotide excision repair are fully capable of somatic hypermutation of immunoglobulin genes. *J. Exp. Med.* 186:413–419.
11. Wagner, S., J. Elvin, P. Norris, J. McGregor, and M. Neuberger. 1996. Somatic hypermutation of Ig genes in patients with xeroderma pigmentosum (XP-D). *Int. Immunol.* 8:701–705.
12. Shen, H.M., D.L. Cheo, E. Friedberg, and U. Storb. 1997. The inactivation of the XP-C gene does not affect somatic hypermutation or class switch recombination of immunoglobulin genes. *Mol. Immunol*. 34:527–533.
13. Jacobs, H., Y. Fujita, G. van der Horst, J. de Boer, G. Weeda, J. Essers, N. de Wind, B. Engelward, L. Samson, S. Verbeek, et al. 1998. Hypermutation of immunoglobulin genes in memory B cells of DNA repair-deficient mice. *J. Exp. Med.* 187:1735–1743.
14. Winter, D., Q. Phung, A. Umar, S. Baker, R. Tarone, R. Tanaka, R. Liskay, T. Kunkel, V. Bohr, and P. Gearhart. 1998. Altered spectra of hypermutation in antibodies from mice deficient for the DNA mismatch repair protein PMS2. *Proc. Natl. Acad. Sci. USA*. 95:6953–6958.
15. Friedberg, E., G. Walker, and W. Siede. 1995. DNA Repair and Mutagenesis. ASM Press, Washington, DC.
16. Modrich, P. 1991. Mechanisms and biological effects of mismatch repair. *Annu. Rev. Genet.* 25:229–253.
17. Baker, S.M., C.E. Bronner, L. Zhang, A.W. Plug, M. Robatzek, G. Warren, E.A. Elliott, J. Yu, T. Ashley, N. Arnheim, et al. 1995. Male mice defective in the DNA mismatch repair gene PMS2 exhibit abnormal chromosome synapsis in meiosis. *Cell*. 82:309–319.
18. Baker, S.M., A.W. Plug, T.A. Prolla, C.E. Bronner, A.C. Harris, X. Yao, D.-M. Christie, C. Monell, N. Arnheim, A. Bradley, et al. 1996. Involvement of mouse Mlh1 in DNA mismatch repair and meiotic crossing over. *Nat. Genet.* 13: 336–342.
19. de Wind, N., M. Dekker, A. Berns, M. Radman, and H. te Riele. 1995. Inactivation of the mouse MSH2 gene results in mismatch repair deficiency, methylation tolerance, hyperrecombination, and predisposition to cancer. *Cell.* 82:321–330.
20. Phung, Q., D. Winter, A. Cranston, R. Tarone, W. Bohr, R. Fishel, and P. Gearhart. 1998. Increased hypermutation at G and C nucleotides in immunoglobulin variable genes from mice deficient for the MSH2 mismatch repair protein. *J. Exp. Med.* 187:1745–1751.
21. Rada, C., M.R. Ehrenstein, M.S. Neuberger, and C. Milstein. 1998. Hot spot focusing of somatic hypermutation in MSH2-deficient mice suggests two stages of mutational targeting. *Immunity*. 9:135–141.
22. Frey, S., B. Bertocci, F. Delbos, L. Quint, J.-C. Weill, and C.-A. Reynaud. 1998. Mismatch repair deficiency interferes with the accumulation of mutations in chronically stimulated B cells and no with the hypermutation process. *Immunity*. 9:127–134.
23. Rogerson, B. 1995. Somatic hypermutation of VHS107 genes is not associated with gene conversion among family members. *Int. Immunol.* 7:1225–1235.
24. Klotz, E., J.J. Hackett, and U. Storb. 1998. Somatic hypermutation of an artificial test substrate within an Ig kappa transgene. *J. Immunol.* 161:782–790.
25. Orita, M., H. Iwahana, H. Kanazawa, K. Hayashi, and S. Takao. 1989. Detection of polymorphism of human DNA by gel electrophoresis as single-strand conformation polymorphism. *Proc. Natl. Acad. Sci. USA*. 86:2766–2770.
26. Storb, U., E. Klotz, J. Hackett, K. Kage, G. Bozek, and T.E. Martin. 1998. A hypermutable insert in an immunoglobulin transgene contains hotspots of somatic mutation and sequences predicting highly stable structures in the RNA transcript. *J. Exp. Med.* 188:689–698.
27. Phung, Q., D. Winter, R. Alrefai, and P. Gearhart. 1999. Hypermutation in Ig V genes from mice deficient in the MLH1 mismatch repair protein. *J. Immunol.* 162:3121–3124.
28. Vora, K., K. Tuma-Brundage, V. Lentz, A. Cranston, R. Fishel, and T. Manser. 1999. Severe attenuation of the B cell immune response in Msh2-deficient mice. *J. Exp. Med.* 189: 471–481.
29. Kim, N., and U. Storb. 1998. The role of DNA repair in somatic hypermutation of immunoglobulin genes. *J. Exp. Med.* 187:1729–1733.
30. Mellon, I., D. Rajpal, M. Koi, C. Boland, and G. Champe. 1996. Transcription-coupled repair deficiency and mutations in human mismatch repair genes. *Science*. 272:557–560.
31. Mellon, I., and G.N. Chanpe. 1996. Products of DNA mismatch repair genes mutS and mutL are required for transcription-coupled nucleotide-excision repair of the lactose operon in *Escherichia coli*. *Proc. Natl. Acad. Sci. USA*. 93:1292–1297.
32. Cascalho, M., J. Wong, C. Steinberg, and M. Wabl. 1998. Mismatch repair co-opted by hypermutation. *Science*. 279: 1207–1210.
33. Park, K., J. Kim, H.-S. Kim, and H.S. Shin. 1998. Isolated human germinal center centroblasts have an intact mismatch repair system. *J. Immunol.* 161:6128–6132.